Multistep Direct Reactions: A Microscopic Two-Component Approach

A. J. Koning
Netherlands Energy Research Foundation ECN,
BU - Nuclear Energy, P.O. Box 1, 1755 ZG Petten, The Netherlands

M. B. Chadwick
University of California, Theoretical Division,
Los Alamos National Laboratory, Los Alamos, NM 87545, USA

Abstract

We present a multistep direct reaction theory for analyzing nucleon-induced reactions to the continuum for incident energies up to 200 MeV. Two principal advances in multistep direct theory are studied: (1) A microscopical approach for calculating DWBA transitions to the continuum, where transitions to all accessible 1p1h shell model states are explicity determined; (2) A two-component formulation of multistep direct reactions is given, where neutron and proton excitations are explicitly accounted for in the evolution of the reaction, for all orders of scattering. The multistep direct theory is applied, along with theories for multistep compound, compound, and collective reactions, to analyze experimental emission spectra for a range of targets and energies. The sensitivity to the employed optical model is demonstrated. We show that the theory correctly accounts for measured neutron and proton emission angle-integrated spectra, as well as angular distributions. Additionally, we note that these microscopic and two-component developments facilitate more fundamental studies into effective nucleon-nucleon interactions in multistep calculations. A more complete exposition of this work can be found in Ref. [1].

1 Introduction

The preequilibrium nuclear reaction mechanism constitutes the bridge between fast, direct processes and slow compound processes, and accounts for the high-energy tails in emission spectra and the smooth forward-peaked angular distributions. In recent years quantum mechanical theories have been developed to describe these mechanisms [2, 3, 4], and the advent of fast computers has enabled numerical computations of these cross sections. Although some controversies regarding the underlying quantum statistics in multistep reactions still exist (such as causality issues in the MSD theory of Feshbach, Kerman, and Koonin [5, 6]), quantum mechanical preequilibrium theories tend to account for experimental angle-integrated emission spectra with an accuracy comparable to that found in the semiclassical models, and with a higher accuracy for angular distributions.

In cases where direct reactions account for scattering to low-lying discrete states, it is natural to expect that such direct-like mechanisms persist in the continuum. An extension of discrete direct reactions to this continuum part of the spectrum is then provided by the multistep direct (MSD) model (where in the term "MSD" the important one-step direct cross section is included). When a reaction proceeds by the MSD mechanism, it is imagined that at least one particle is in the continuum throughout the process and that at each subsequent step of the reaction a new particle-hole pair is created. After one or a few collisions, the continuum particle is emitted in a direction that still has retained some coupling to the initial direction and is therefore forward-peaked. The main difference with conventional direct reaction

theories is the high density of final and intermediate states, which necessitates statistical postulates in the direct reaction formalism so that the analysis of these processes remains tractable. A comparison of both the theoretical [7] and practical [8] aspects of several MSD models revealed that the model of Feshbach, Kerman and Koonin (FKK) [5], derived using a statistical assumption called leading-particle statistics, is computationally the most attractive model because of its convolution structure.

In this paper we present a formalism for calculating MSD cross sections in a fully two-component theory where all possible neutron and proton particle-hole excitations are explicitly followed, for all orders of scattering. While this may at first seem to be a formidable task, especially for multistep processes where the many possible reaction pathways becomes large in a two-component formalism, we show that this is not so – a rather simple generalization of the FKK convolution expression automatically generates these pathways. Such considerations are particularly relevant when simultaneously analyzing both neutron and proton emission spectra, which is always important since these processes represent competing decay channels.

We also study a new, and fully microscopic, method for calculating MSD cross sections which does not make use of particle-hole state densities but instead directly calculates cross sections for all possible particle-hole excitations (again including an exact book-keeping of the neutron/proton type of the particle and hole at all stages of the reaction) determined from a simple non-interacting shell model. This is in contrast to all previous numerical implementations of the FKK theory which sample only a small number of such states to estimate the DWBA strength, and utilize simple analytical formulae for the partial state density, based on the equidistant spacing model.

2 Theory

The double-differential MSD cross section to the continuum is an incoherent sum of a one-step term and multistep terms,

$$\frac{d^2\sigma_{j\leftarrow i}(E,\Omega\leftarrow E_0,\Omega_0)}{d\Omega dE} = \sum_{n=1}^{\infty} \frac{d^2\sigma^{(n)}_{j\leftarrow i}(E,\Omega\leftarrow E,\Omega_0)}{d\Omega dE}, \tag{1}$$

where E_0, Ω_0, i and E, Ω, j are the energy, solid angle and type of the incident and outgoing nucleon, respectively. Using the methodology and notation of Refs. [4, 7], the different terms of the MSD cross section can be rewritten into a form that enables excited neutrons and protons to be distinguished and followed throughout all scattering stages.

2.1 The one-step cross section

The continuum one-step direct cross section is a weighted sum over squared DWBA matrix elements that describe transitions to particle-hole states μ. In a two-component form, it is given by

$$\begin{aligned}\frac{d^2\sigma^{(1)}_{j\leftarrow i}(E,\Omega\leftarrow E_0,\Omega_0)}{d\Omega dE} &= \frac{m^2}{(2\pi\hbar^2)^2}\frac{k}{k_0}\sum_{\mu}\hat{\rho}_{\mu}(p_\pi,h_\pi,p_\nu,h_\nu,E_x) \\ &\times \left|\langle\chi^{(-)}_j(E,\Omega)|\langle\mu(p_\pi,h_\pi,p_\nu,h_\nu)|\mathcal{V}|0\rangle|\chi^{(+)}_i(E_0,\Omega_0)\rangle\right|^2, \end{aligned}\tag{2}$$

where k and k_0 are the final and initial momentum and $E_x = E_0 - E + Q$ is the excitation energy with Q the reaction Q-value. The distorted waves χ are eigenfunctions of the Schrödinger equation with an optical potential. The effective nucleon-nucleon interaction $\mathcal{V}$ serves as a scaling factor in MSD calculations and manifests itself in $\mathcal{V}_{\pi\pi}$, $\mathcal{V}_{\pi\nu}$ $(= \mathcal{V}_{\nu\pi})$ and $\mathcal{V}_{\nu\nu}$ components. The contribution of each particle-hole state to the continuum is determined by the $1p1h$-distribution $\hat{\rho}_\mu$ [7].

As we consider incident and outgoing nucleons in this paper, it is instructive to give the expression for a charge exchange reaction. In a (p,n) reaction, the excited particle-hole pair is necessarily of the (1,0,0,1) type and the effective interaction is $\mathcal{V}_{\pi\nu}$. Hence, Eq. (2) becomes

$$\frac{d^2\sigma^{(1)}_{\nu\leftarrow\pi}(E,\Omega\leftarrow E_0,\Omega_0)}{d\Omega dE} = \frac{m^2}{(2\pi\hbar^2)^2}\frac{k}{k_0}\sum_{\mu}\hat{\rho}_{\mu}(1,0,0,1,E_x)$$

$$\times \quad |\langle \chi_\nu^{(-)}(E,\Omega)|\langle \mu(1,0,0,1)|\mathcal{V}_{\pi\nu}|0\rangle|\chi_\pi^{(+)}(E_0,\Omega_0)\rangle|^2. \tag{3}$$

An analogous equation applies for an (n,p) reaction where the configuration is (0,1,1,0). In a (p,p') reaction, both (1,1,0,0) and (0,0,1,1) pairs can be excited and both $\mathcal{V}_{\pi\pi}$ and $\mathcal{V}_{\pi\nu}$ are involved.

2.2 The multistep cross section

The derivation of the two-step FKK cross section from the continuum distorted wave theory is by no means trivial and has led to a certain amount of controversy [4, 6, 9]. The complete derivation is given in [4]. When we repeat this while distinguishing between neutrons and protons, there appears an extra summation over t_1, indicating both types of intermediate nucleons,

$$\begin{aligned}\frac{d^2\sigma^{(2)}_{j\leftarrow i}(E,\Omega\leftarrow E_0,\Omega_0)}{d\Omega dE} &= \frac{2m^5}{(2\pi)^8\hbar^{10}}\frac{k}{k_0}2\pi^2\sum_{t_1=\pi,\nu}\sum_{\mu}\sum_{\mu'}\int \mathrm{d}\Omega_1\int \mathrm{d}E_1E_1\\
&\times \ \hat{\rho}_{\mu'}(p_\pi,h_\pi,p_\nu,h_\nu,E_x'')\hat{\rho}_{\mu}(p_\pi,h_\pi,p_\nu,h_\nu,E_x')\\
&\times \ |\langle \bar{\chi}_j^{(-)}(E,\Omega)|\langle \mu'(p_\pi,h_\pi,p_\nu,h_\nu)|\mathcal{V}|0\rangle|\bar{\chi}_{t_1}^{(+)}(E_1,\Omega_1)\rangle|^2\\
&\times \ |\langle \bar{\chi}_{t_1}^{(-)}(E_1,\Omega_1)|\langle \mu(p_\pi,h_\pi,p_\nu,h_\nu)|\mathcal{V}|0\rangle|\bar{\chi}_i^{(+)}(E_0,\Omega_0)\rangle|^2,\end{aligned} \tag{4}$$

where E_1,Ω_1 are the intermediate energy and solid angle, respectively, and E_x' and E_x'', are the excitation energies at each stage.

The sum over t_1 in Eq. (4) indicates that the number of possible scattering terms is larger compared to the one-component approach. Nevertheless, the attractive convolution structure remains present in the two-component approach. Indeed, combining Eq. (2) and Eq. (4) gives

$$\begin{aligned}\frac{d^2\sigma^{(2)}_{j\leftarrow i}(E,\Omega\leftarrow E_0,\Omega_0)}{d\Omega dE} &= \frac{m}{4\pi^2\hbar^2}\sum_{t_1=\pi,\nu}\int \mathrm{d}\Omega_1\int \mathrm{d}E_1E_1\\
\times \quad \frac{d^2\sigma^{(1)}_{j\leftarrow t_1}(E,\Omega\leftarrow E_1,\Omega_1)}{d\Omega dE}&\frac{d^2\sigma^{(1)}_{t_1\leftarrow i}(E_1,\Omega_1\leftarrow E_0,\Omega_0)}{d\Omega_1 dE_1}.\end{aligned} \tag{5}$$

This method can be extended to the higher steps. In general, the n-step direct cross section can be completely expressed in terms of the two-component MSD cross section of the previous stage

$$\begin{aligned}\frac{d^2\sigma^{(n)}_{j\leftarrow i}(E,\Omega\leftarrow E_0,\Omega_0)}{d\Omega dE} &= \frac{m}{4\pi^2\hbar^2}\sum_{t_{n-1}=\pi,\nu}\int \mathrm{d}\Omega_{n-1}\int \mathrm{d}E_{n-1}E_{n-1}\\
\times \quad \frac{d^2\sigma^{(1)}_{j\leftarrow t_{n-1}}(E,\Omega\leftarrow E_{n-1},\Omega_{n-1})}{d\Omega dE}&\frac{d^2\sigma^{(n-1)}_{t_{n-1}\leftarrow i}(E_{n-1},\Omega_{n-1}\leftarrow E_0,\Omega_0)}{d\Omega_1 dE_1}.\end{aligned} \tag{6}$$

Note that in this multistep description, we do not make the approximation that the *same* leading-particle is followed throughout the scattering sequence. In line with the general MSD picture, our summation over both intermediate neutrons and protons assures that at least one particle is in the continuum throughout the multistep process. In addition, the convolution structure of the two-component multistep formula automatically generates all possible cross-terms involving various types of excited particle-hole states and leading particles.

In sum, although the number of possible paths quickly increases for the higher steps, the convolution structure automatically takes care of the book-keeping.

3 DWBA calculations

The aforementioned formalism indicates that a significant part of an MSD analysis consists of the computation of DWBA cross sections for transitions to particle-hole states. To obtain these $1p1h$-states,

single-particle states are generated with a simple Nilsson model. With this model, a set of both proton and neutron single-particle states can be created. In our DWBA calculations, we include only the particle-hole pairs that obey parity and angular momentum conservation. Consequently, only normal-parity states are included. This is consistent with our choice to consider a nucleon-nucleon interaction that consists of only a real, central term (see below).

All DWBA matrix elements are calculated with the nuclear reaction code ECIS95 [10]. The scattering states are computed using an optical model potential, which we discuss later when we look at some specific reactions. We only consider the real, central term of the effective nucleon-nucleon interaction $\mathcal{V}_{ij}$, for which we take a Yukawa potential with range $r_0 = 1$ fm and strength V_{ij}. This strength is taken as the only adjustable parameter in our MSD calculations. We determine the bound state wave functions with a Woods-Saxon potential. Its parameters are a reduced radius of 1.2 fm and a diffuseness of 0.6 fm. We take a starting value of 50 MeV for the potential depth and let ECIS95 search for the true value.

For a DWBA calculation with ECIS95, the excitation energy (and not the separate particle and hole energies) needs to be specified. In the present work, we assume that the excited particle is always bound, even if the finite depth of the hole forbids this, due to restrictions in currently available DWBA codes.

Usually, we are interested in the simultaneous calculation of e.g. (p, xn) and (p, xp) spectra and this requires one-step (p, n) reactions (exciting π-particles and ν-holes), (n, n') and (p, p') reactions (exciting both π-particles, π-holes and ν-particles, ν-holes) and one-step (n, p) reactions (exciting ν-particles and π-holes).

It is clear that for our approach, the MSD calculations can get quite involved: a typical computation of 80 MeV (p, xn) and (p, xp) spectra on ^{90}Zr requires more than 60,000 individual DWBA cross section calculations. We mention however that our calculational approach is involved, but tractable because each shell model state is included only once, assuming the state is completely degenerate. The more realistic splitting is then taken into account phenomenologically in an approximate way, by a Gaussian distribution over the particle-hole states after the DWBA calculation.

4 Other reaction models included

Although our work is primarily directed towards reactions to the continuum, we aim at a full treatment of all complementary reaction mechanisms. By combining the direct, pre-equilibrium and compound nuclear models in one calculation we are able to predict double-differential spectra and residual production cross sections [11] for incident energies up to 200 MeV. The code system that performs this task, MINGUS, is schematically given in Fig. 1, which displays the other reaction mechanisms included. It will be clear that MINGUS is completely built around ECIS-95.

Our calculations include direct, discrete effects at low excitation energies. In this way we can avoid a simulation of the collective part of the spectrum by the incoherent continuum MSD mechanism. A method to include these collective effects is described in Refs. [12, 13] and we basically follow that approach here. In order not to miss any collective strength, our calculations include all discrete levels of the nucleus for which the spin, parity and deformation lengths δ_L are known.

Multi-step compound (MSC) reactions occur for incident energies up to a few tens of MeV. In the MSC reaction mechanism, the stepwise reaction proceeds through the bound configurations of the composite nucleus. As with compound reactions, it is imagined that the incident particle is captured by the target nucleus but that emission takes place before the attainment of statistical equilibrium. For MSC reactions, we employ the model of Feshbach, Kerman and Koonin [5]. Our implementation of the FKK formalism essentially follows the method of Chadwick and Young [14].

We describe primary compound emission by the continuum Hauser-Feshbach formula. and use the Weisskopf-Ewing model for compound reactions after the first stage. For the total level density $\omega(E_x)$ we take the composite formula as proposed by Gilbert and Cameron [15] and incorporate shell effects in our calculations by adopting the method of Ignatyuk [16] for the level density parameter a.

For incident energies below about 50 MeV, one can safely assume that after primary pre-equilibrium emission the excitation energy of the residual nucleus is relatively small and that further decay of the nucleus proceeds by a pure compound mechanism. At higher incident energies such an assumption will

result in an underprediction of the outgoing spectrum above the evaporation peak. This deficit stems from the omission of multiple pre-equilibrium emission: it is conceivable that after the first reaction the residual excitation energy is so high that another fast particle can be emitted before equilibration of the nucleus. To include this, we adopt the multiple MSD method of Ref. [17].

5 Comparison with experimental data

Comparisons between pre-equilibrium models and experimental data have been performed in the energy region 10-200 MeV. Many examples can be found in [1]. Here, we have chosen the 80 MeV double-differential (p,xp) and (p,xn) reactions on ^{90}Zr to demonstrate the sensitivity to the optical model and level density parameters. The comparison of the fully microscopical approach with experimental data as displayed in Fig. 2a is obtained with Madland's optical model [18] above 50 MeV and the Becchetti-Greenlees parametrization [19] below 50 MeV. This results in a sizeable overestimation at the backward angles, even at an outgoing energy of 60 MeV. In Fig. 3 we show the same reaction but now predicted using Menet's potential [20] above 20 MeV and Becchetti-Greenlees [19] below 20 MeV. This optical model choice clearly improves the fit, although not yet to a satisfactory level. The calculated angular distribution changes significantly if we use an approach with state densities. Fig. 2b shows the same reaction, again with the Madland and Becchetti-Greenlees potential and with the same set of DWBA matrix elements, but now with Betak and Dobes' formula [21] for the $1p1h$ state density and a constant spin cutoff factor [22]. There is now excellent agreement with experiment. The reason is that in the fully microscopic approach, individual DWBA cross sections for several high-spin states give a rather flat contribution to the total sum, resulting in a less forward peaked angular distribution. When partial state densities are used, the involved Wigner-type spin distribution strongly inhibits the contribution of these averaged DWBA cross sections for high J, leading to a good prediction in this specific case. The same reaction has been analyzed within one-component approaches Refs. [8, 17, 23], where also good agreement is found using these simple equidistant spacing model expression. Fig. 2c shows the effect of applying an energy dependent spin cutoff factor [24]. As expected, this leads to a flatter angular distribution. One should, at this stage, be cautious in drawing conclusions from this spin distribution phenomenon since at least two uncertainties remain: First, the examples show that the dependence on the use of the particular global optical model is rather sensitive. Dedicated optical potentials for ^{90}Zr for the whole energy region of interest (of which we are unaware) should reduce this uncertainty. Second, a significant fraction of the particle-hole states around an excitation energy of 20 MeV are unbound - in our calculations they are assumed to be quasi-bound - and the influence of these transitions is still unknown. The angle-integrated (p,xn) and (p,xp) spectra are well predicted, see Figs. 3a-b and we note that the angle-integrated spectra are less sensitive to the optical model choice. We used the optical model of Walter and Guss [25] for neutrons. Note that at an outgoing energy of 20 MeV there is a sizeable contribution from multiple MSD emission. For all reactions above 60 MeV, we assume $V_{\pi\nu} = V_{\pi\pi} = V_{\nu\nu}$. Next, MINGUS determines this value using the unitarity requirement.

We used the values for $V_{\pi\nu}$ to obtain the following, incident energy dependent, expression

$$V_{\pi\nu} = 31.8 \exp(-\frac{0.20}{31.8}E) \tag{7}$$

which is similar to the simpler one-component V_0-results [2]

This energy dependence for the strength of the effective interaction is included in MINGUS, so that for lower incident energies that appear for the higher steps, consistent values are taken.

6 Conclusions and future work

We have presented a new model for the computation of multistep direct reactions. The theoretical improvement consists of an extension of the MSD formalism to a model that distinguishes between protons and neutrons for both the leading particle and the excited particles and holes for all orders of scattering. Our formalism enables both completely microscopical calculations, in which all particle-hole

states as predicted by the shell model are included, and an approximate approach using partial state densities and averaged DWBA cross sections. We have adopted the FKK model for the second and higher steps. In the two-component approach, the attractive convolution structure of the multistep cross section remains present, though an extra summation over intermediate neutrons and protons appears. Particle-hole states are generated with a spherical Nilsson model and each individual $1p1h$-state is spread over the energy spectrum using a Gaussian distribution. For fully microscopic calculations, these states are then adopted for our MSD model.

All complementary reaction models, namely direct, MSC and compound are included. Comparisons of MINGUS calculations with measurements illustrate the sensitivity of the results to the optical models and the shape of the spin distribution. Allowing ourselves the adjustment of one parameter, the (ratio of the) strength of the effective interaction, we obtain a globally good description of experimental double-differential continuum spectra.

Although our method removes several existing uncertainties within MSD approaches, we appreciate that many aspects still need to be explored:

- **Spin transfer reactions and the nucleon-nucleon itnteraction**. We have only included normal parity states in our analysis, in line with our choice of a simple central form for the effective nucleon-nucleon interaction. An obvious extension is to employ the full expansion of $\mathcal{V}$, including non-central, imaginary and spin-orbit terms.

- **The Tamura-Udagawa-Lenske (TUL) model**. From the theoretical point of view, the multistep method described in this paper can be easily modified to calculate the full multistep matrix element, including all two-component aspects. This would enable a microscopic validation of the TUL model [26] With regard to the MSD literature of the past decade, the TUL model is perhaps less controversial than the FKK model. The randomness of the distribution amplitudes is the only basic statistical assumption underlying the TUL theory for the higher steps, and has been verified independently in nuclear structure studies [7].

- **Unbound $1p1h$-states**. Recently, the code ECIS has been extended to include the possibility for calculating transitions to unbound particle-hole states. The physical meaning of these calculations and their application in MSD reaction theory is presently under study. Inclusion of these unbound states may lead to more realistic MSD results, especially for multiple MSD emission when more than one continuum particle is present.

- **Adequate optical potentials**. Most calculations in this paper were based on global optical model parametrizations and we have confirmed the sensitivity of the MSD results on the optical model parameters. Optical models especially tailored to the nucleus under consideration would at least reduce another uncertainty of quantum-mechanical pre-equilibrium calculations. Potentials constructed from microscopic information, such as provided by Jeukenne, Lejeune and Mahaux [27], may be most preferable.

- **Multiple pre-equilibrium emission**. The present available method is, although practically very efficient, theoretically not yet at a satisfactory level.

- **Realistic single-particle level schemes and level densities**. Although the equidistant spacing model, that leads to simple analytical expressions, has been quite sucessful for the analysis of pre-equilibrium spectra, we feel that realistic single-particle level schemes would provide the MSD method with a more physical basis. Both for a fully microscopic approach and for an approach using state densities, level schemes built from fundamental nucleon-nucleon interactions should be preferred.

Ideally, an MSD analysis should include the most sophisticated ingredients from other independent nuclear structure/reaction studies, so that uncertainties in the cross section calculations can be reduced, facilitating a better test of the underlying quantum statistical assumptions. In the present context, this means use of a level density prescription based on a realistic microscopical level scheme, as much discrete level information as possible, high-quality optical models and a state-of-the-art prescription of the nucleon-nucleon interaction.

References

[1] A.J. Koning and M.B. Chadwick, submitted to Phys. Rev. **C**.

[2] E. Gadioli and P.E. Hodgson, *Pre-equilibrium reactions* (Clarendon, Oxford, 1992).

[3] R. Bonetti, M.B. Chadwick, P.E. Hodgson, B.V. Carlson and M.S. Hussein, Phys. Rep. **202**, no. 4, 171 (1991).

[4] R. Bonetti, A.J. Koning, J.M. Akkermans and P.E. Hodgson, Phys. Rep. **247**, no.1, 1 (1994).

[5] H. Feshbach, A. Kerman and S. Koonin, Ann. Phys. (NY) **125**, 429 (1980).

[6] *Multistep Direct Reactions*, Faure, South Africa, ed. R.H. Lemmer, World Scientific (1992), contributions by H. Feshbach, P.E. Hodgson, A.J. Koning and J.M. Akkermans.

[7] A.J. Koning and J.M. Akkermans, Ann. Phys. (NY) **208**, no.1, 216 (1991).

[8] A.J. Koning and J.M. Akkermans, Phys. Rev. **C47**, 724 (1993).

[9] M.B. Chadwick, P.G. Young and F.S. Dietrich, *Intermediate Energy Nuclear Data: Models and Codes*, Issy-les-Moulineaux, France (1994), 67.

[10] J. Raynal, *Notes on ECIS94*, CEA Saclay report CEA-N-2772 (1994).

[11] R. Michel and P. Nagel, *International code comparison for Intermediate Energy Activation Yields*, NEA report, to be published, 1996.

[12] A.J. Koning, O. Bersillon and J.-P. Delaroche, *Intermediate Energy Nuclear Data: Models and Codes*, Issy-les-Moulineaux, France (1994), 87.

[13] A.J. Koning, O. Bersillon and J.-P. Delaroche, *International Conference on Nuclear Data for Science and Technology*, Gatlinburg, USA (1994), 1072.

[14] M.B. Chadwick and P.G. Young, Phys. Rev. **C47**, 2255 (1993).

[15] A. Gilbert and A.G.W. Cameron, Can. J. Phys. **43**, 1446 (1965).

[16] A.V. Ignatyuk, G.N. Smirenkin and A.S. Tishin, Sov. J. Nucl. Phys. **21**, no. 3, 255 (1975).

[17] M.B. Chadwick, P.G. Young, D.C. George and Y. Watanabe, Phys. Rev. **C50**, 996 (1994).

[18] D.G. Madland, in *Proceedings of a Specialists' Meeting on Preequilibrium Reactions*, Semmering, Austria, februari 10-12 1988, edited by B. Strohmaier (OECD, Paris 1988), p. 103; Internationl Atomic Energy Agency Report No. IAEA-TECDOC-483, 1988, p. 80 (unpublished).

[19] F.D. Becchetti and G.W. Greenlees, Phys. Rev. **C182**, 1190 (1969).

[20] J.J.H. Menet, E.E. Gross, J.J. Malanify and A.Zucker Phys. Rev. **C4**, 1114 (1971).

[21] E. Betak and J. Dobes, Z. Phys. **A279**, 319 (1976).

[22] H. Gruppelaar, *IAEA Advisory Group Meeting on Basic and Applied Problems on Nuclear Level Densities* (Brookhaven National Laboratory report, 1983), 143.

[23] A.A. Cowley et al., Phys. Rev. **C43**, 678 (1991).

[24] M. Herman and G. Reffo, *OECD Meeting on Nuclear level densities*, Bologna, Italy (1989), 103.

[25] R.L. Walter and P.P. Guss, in *Nuclear Data for Basic and Applied Science*, Santa Fe, 1985, edited by P.G. Young (Gordon and Breach, N.Y., 1986), p. 1079.

[26] T. Tamura, T. Udagawa and Lenske, Phys. Rev. **C26**, 379 (1982).

[27] J.-P. Jeukenne, A. Lejeune and C. Mahaux, Phys. Rev. **C16**, 80 (1977).

[28] M. Trabandt et al., Phys. Rev. **C39**, 452 (1989).

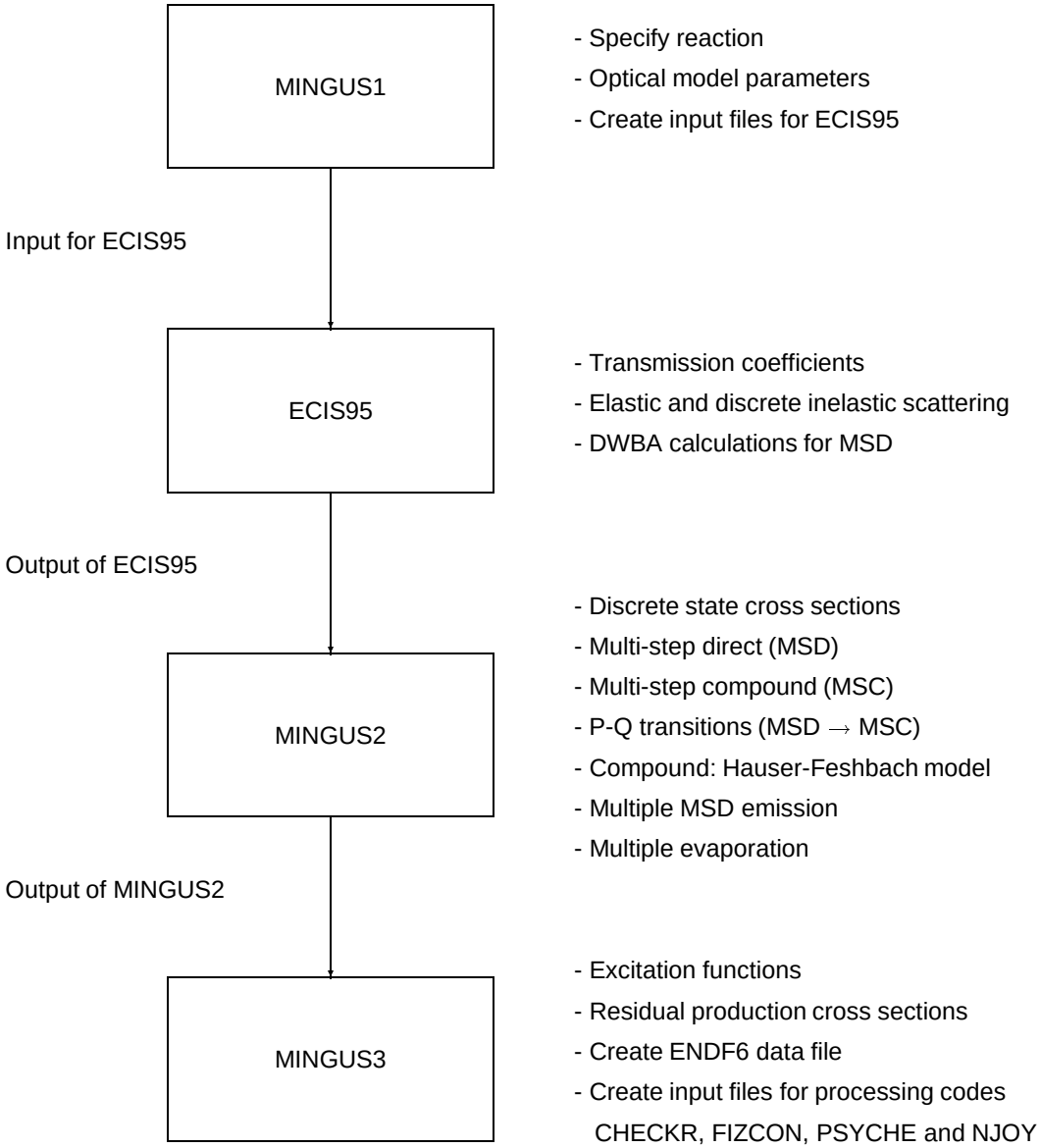

Figure 1: Flow chart of the nuclear model code system MINGUS

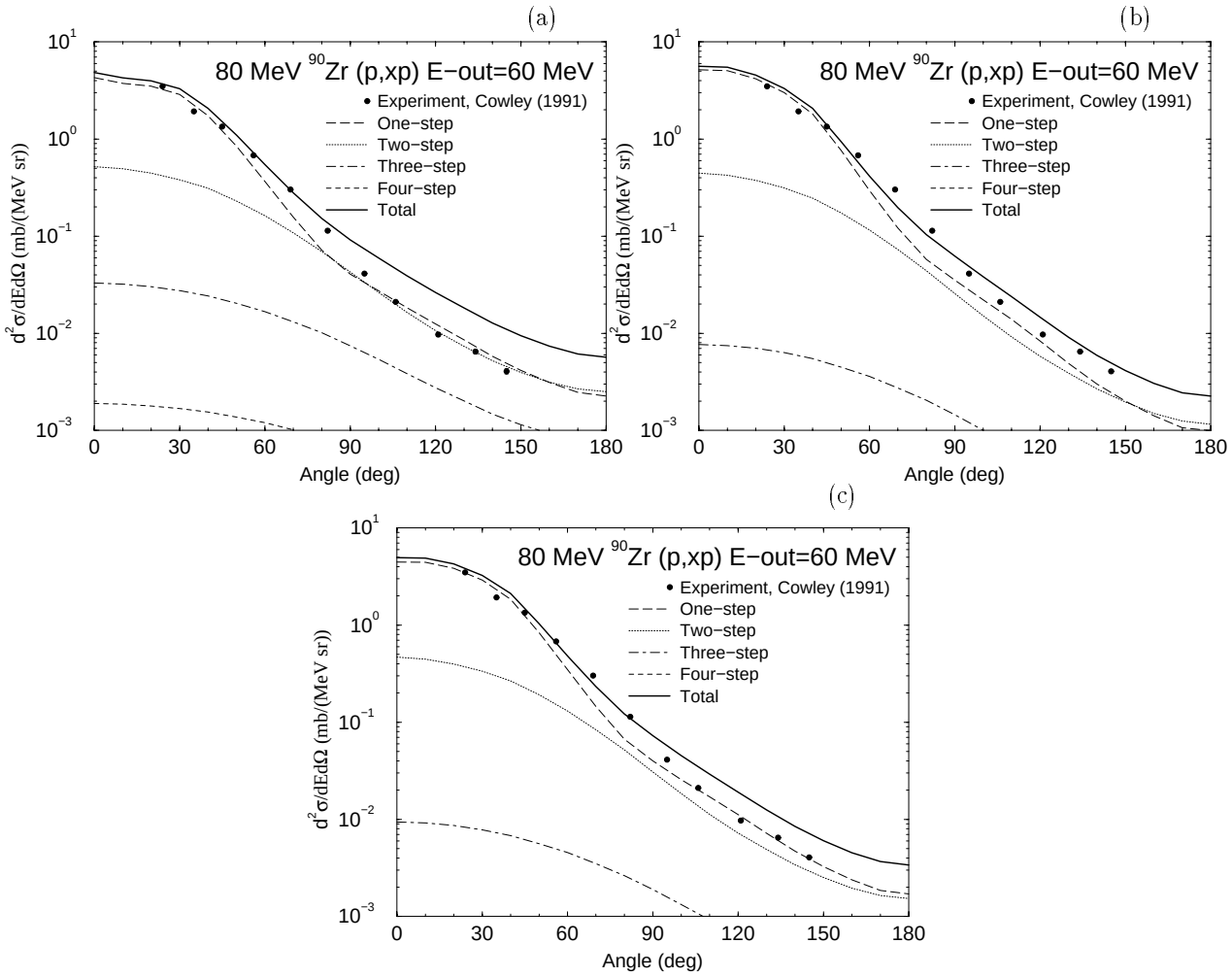

Figure 2: Comparison of calculated double-differential cross sections, using the potentials of Madland [18] and Becchetti-Greenlees [19], with experimental data for 80 MeV ^{90}Zr (p, xp) [23] at an outgoing energy of 60 MeV: (a) fully microscopic, (b) state density-based calculations with a constant spin cutoff factor [22] and (c) with an energy dependent spin cutoff factor [24]

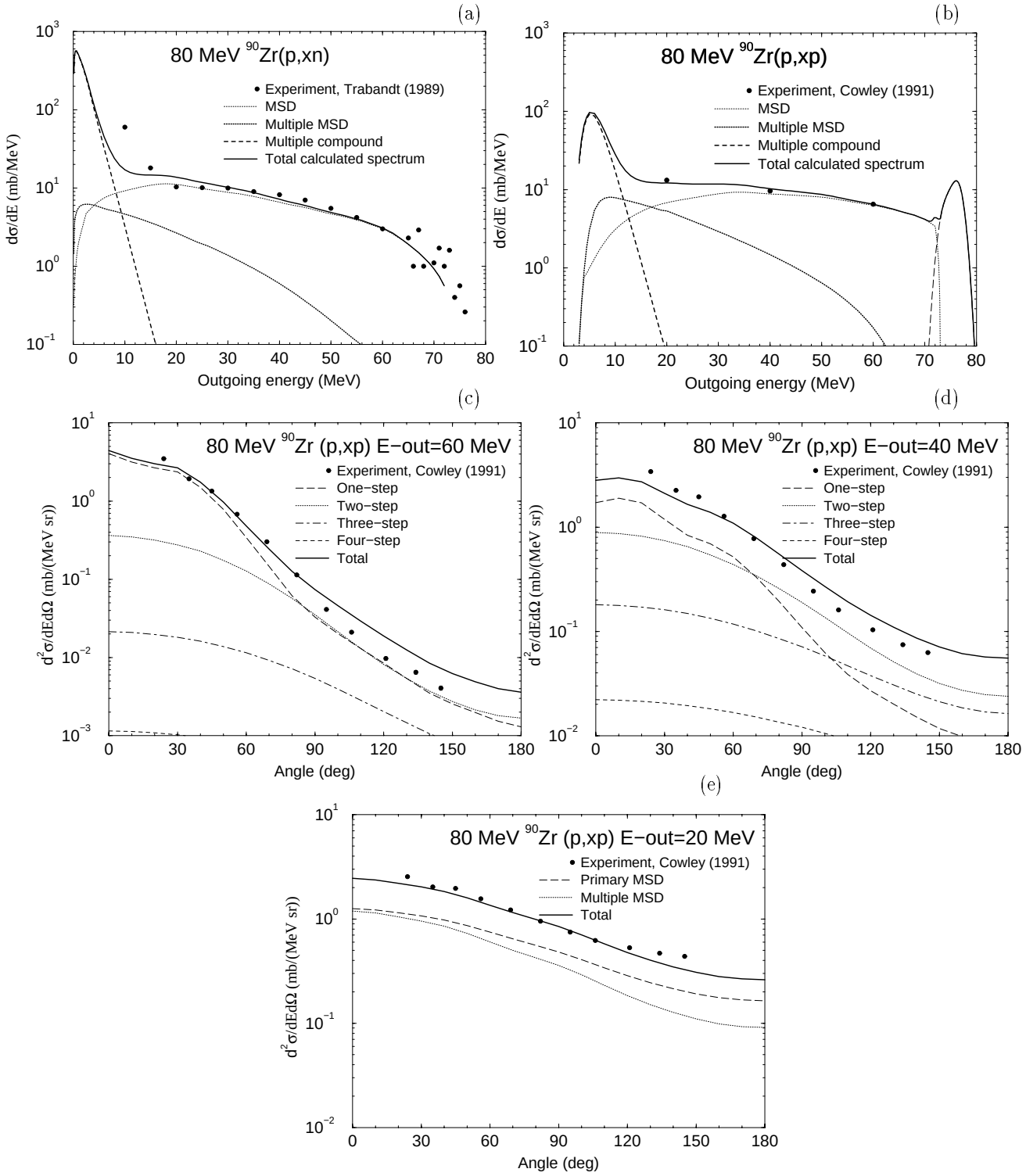

Figure 3: Comparison of fully microscopical calculations, with the potentials of Menet [20] and Becchetti-Greenlees [19], with experimental data for 80 MeV protons on ^{90}Zr: (a) angle-integrated (p, xn) cross section [28], (b) angle-integrated (p, xp) cross section. Double-differential (p, xp) cross section at outgoing energies of (c) 60 MeV, (d) 40 MeV and (e) 20 MeV.